Journal of Applied Mathematics and Physics, 2025, 13(4), 1523-1544
https://www.scirp.org/journal/jamp
ISSN Online: 2327-4379
ISSN Print: 2327-4352

Viscoelastic Bending Analysis of Inhomogeneous Fiber-Reinforced Moderately Thick Sandwich Plates

Hamada Fawzy El-Mekawy[1*], Ashraf M. Zenkour[2,3]

[1]Department of Management Information Systems, College of Business and Economics, Qassim University, Buraidah, Saudi Arabia
[2]Department of Mathematics, Faculty of Science, King Abdulaziz University, Jeddah, Saudi Arabia
[3]Department of Mathematics, Faculty of Science, Kafrelsheikh University, Kafrelsheikh, Egypt
Email: *hamf.halawa@qu.edu.sa

How to cite this paper: El-Mekawy, H.F. and Zenkour, A.M. (2025) Viscoelastic Bending Analysis of Inhomogeneous Fiber-Reinforced Moderately Thick Sandwich Plates. *Journal of Applied Mathematics and Physics*, **13**, 1523-1544.
https://doi.org/10.4236/jamp.2025.134082

Received: March 27, 2025
Accepted: April 24, 2025
Published: April 27, 2025

Abstract

A higher-order shear deformation plate theory is used to study the bending response of inhomogeneous viscoelastic sandwich plates. Several kinds of sandwich plates are considered taking into account the symmetry of the plate and the thickness of each layer. The effective moduli and Il'yushin's approximation methods are used to solve the equations governing the bending of simply supported inhomogeneous fiber-reinforced viscoelastic sandwich plates. Numerical results for deflections and stresses are presented. The effects due to time parameter, aspect ratio, side-to-thickness ratio, and constitutive parameter are investigated.

Keywords

Il'yushin's Method, Inhomogeneous, Sandwich Plates, Viscoelastic

1. Introduction

Composite structures are widespread in aerospace, automotive, and marine industries, and several plate theories have been developed to analyze deformations of composite plates. A sandwich structure consists of three distinct layers (i.e., the top face, the core, and the bottom face), which are bonded together to form an efficient load-carrying assembly. During the past decade, Sandwich plates have been increasingly used in civil engineering structures, due to their high strength-to-weight ratio.

The classical Kirchhoff thin plate theory (CLT), which ignores transverse shear effects, provides reasonable results for thin plates. However, it may not give accurate results for moderately thick plates. An improvement on the CLT is the first-order shear deformation theory (FSDT), such as the Reissner-Mindlin theory, which accounts for transverse shear effects but needs a shear correction factor. Higher-order shear deformation plate theories are those in which the displacements are expanded up to quadratic or higher powers of the thickness coordinate and can be used to compute inter-laminar stresses more accurately and do not require shear correction factors. The first scientists that developed the theories of plates and shells were Hildebrand *et al.* [1]. Nelson and Lorch [2] and Librescu [3] presented higher-order displacement-based shear deformation theories for the analysis of laminated plates. Lo *et al.* [4] [5] have presented a closed-form solution for a laminated plate with a higher-order displacement model, which also considers the effect of transverse normal deformation. Various higher-order theories that lead to a parabolic distribution of transverse strain through the thickness have also been developed [6] [7]. Of all the higher-order theories, the one proposed by Reddy [8]-[10] was the first to obtain the equilibrium equations consistently using the principle of virtual displacements. Zenkour investigated deflection, buckling, and free vibration [11] [12] using various plate theories.

The rapid development of the industry motivated the development of more general and rigorous plate theories to offer a better representation of the kinematics of plates. So, the transient behavior of composite plates has long been a main subject of many studies. However, these studies are limited to the response of homogeneous composite plates. Even the few studies accounting for the structural response of non-homogeneous composite plates deal with special cases of non-homogeneity and anisotropy, and the reported results in open literature are rare [13]-[17]. Various theories of homogeneous laminated plates [16] are extended to the non-homogeneous ones. Fares and Zenkour [18] devoted to the free vibration and buckling problems of non-homogeneous composite plates. Fares and Zenkour [19] used a higher-order theory to investigate the response of non-homogeneous anisotropic laminated plates. Zenkour and Radwan [20] studied the bending and buckling behaviors of inhomogeneous plates resting on elastic foundations in a hygrothermal location. Ellali *et al.* [21] presented the wave propagation of an inhomogeneous plate via a new integral inverse cotangential shear model with temperature-dependent material properties. Garg *et al.* [22] used the zigzag theory and finite element method to study the free vibration of inhomogeneous sandwich plates in hygrothermal conditions. Garg *et al.* [23] presented a comparative study on the buckling response of exponential, power, and sigmoidal inhomogeneous sandwich plates under hygrothermal conditions.

The viscoelastic core for the analysis of sandwich beams was performed in 1965 by DiTaranto [24] and in 1969 by Mead and Markus [25] due to the beam axis and bending vibration. Several careful phase viscoelastic heterogeneous media with known stress suppression relationships demonstrate that the effective relaxation and creep functions can be obtained through the corresponding principles of the theory of linear viscous flames. Wilson and Vinson [26] discussed the stability of viscoelastic correction plates exposed to biaxial compression.

The viscoelastic load of sandwich panels with cross sherry faces was examined by Kim and Hong [27] and Huang [28]. Dynamic reaction isotropic viscoelastic plates were analyzed by Pan [29]. Librescu and Chandiramani [30] have presented a paper dealing with the dynamic stability analysis of lateral isotropic viscoelastic plates exposed to levels of biaxial edge loading systems. Zenkour [31] examined the quasi-static stability analysis of fiber-reinforced viscoelastic rectangular plates exposed to edge loading systems. Zenkour [32] has investigated the static thermo-viscoelastic responses of fiber-reinforced composite plates using a refined shear deformation theory. Zenkour and El-Shahrany [33] [34] discussed the hygroscopic forced vibration and frequency control of viscoelastic laminate plates equipped with a strict actuator of magnets above viscoelastic foundations. Zenkour [35] discussed the nonlocal thermal vibrations of embedded nanoplates in a viscoelastic medium. Sobhy *et al.* [36] examined hygienic waveform analysis of metal foam microplates reinforced by graphs embedded in a viscoelastic media. Pham *et al.* [37] examined higher-order nonlocal finite element modeling for vibrational analysis of viscoelastic orthotropic nanoplates on top of viscoelastic foundations. Zenkour and El-Mekawy [38] investigated the bending analysis of inhomogeneous elastic/viscoelastic/elastic (e-v-e) sandwich plates using hyperbolic shear deformation theory. Recently, Zenkour *et al.* [39] investigated bending analysis of uniform and heterogeneous viscoelastic sandwich plates using classical plate theory.

In this work, higher-order shear deformation plate theory was investigated for the bending response of inhomogeneous viscoelastic sandwich plates. We will explain two different cases of sandwich plates. In the first (e-v-e) case the core is made from an isotropic viscoelastic material, and the surface is made from an isotropic elastic material, which has the same elastic properties. In the other (v-e-v) case, the core is an isotropic elastic material, and the faces are viscoelastic material with the same viscoelastic modular. Effective-moduli method [40] and Illyushin's approximation method [41] can be used to solve equations that regulate the bending of simply supported, simple fiber-reinforced viscoelastic sandwich plates. Various results are presented. Symmetrical analysis of pathological fiber-reinforced viscoelastic rectangular sandwich panels.

2. Problem Formulation

Consider a flat sandwich plate made up of three microscopically heterogeneous layers (see **Figure 1**). The Cartesian coordinates (x, y, z) of the rectangle are used to describe the infinite deformation of a three-layer sandwich elastic plate occupying the region $x \in [0, a]$, $y \in [0, b]$, and $z = [-h/2, h/2]$ of unknown references.

The intermediate level of the beam is defined by $z = 0$ the outer boundary level is defined by $z = \pm h/2$. The layers of sandwich plate layers are made of isotropic non-uniform materials with material properties that change smoothly only in the z (thickness) direction.

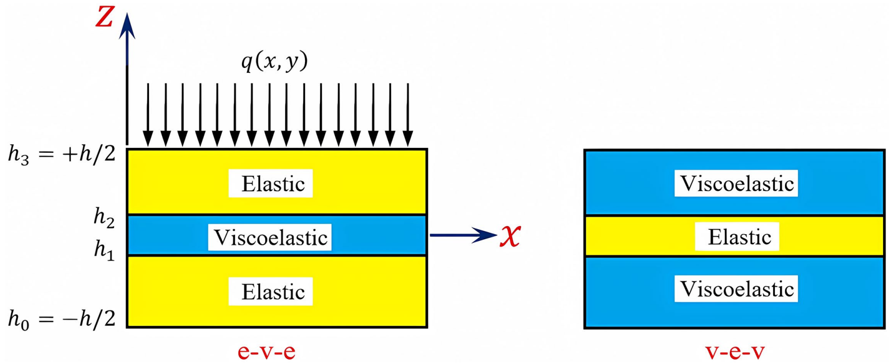

Figure 1. Geometry and coordinate system of viscoelastic sandwich panels.

The effective material properties of any layer, such as Young's modulus, are:

$$E_{(k)}(z) = E_k \mathrm{e}^{-\frac{nz}{h}}, \quad k = 1,2,3. \tag{1}$$

Normal towing $\sigma_z = q(x,y)$ is applied to the top of the top, but no towing is applied to the bottom is applied on the upper surface, The shift of the material point at (x,y,z) of the beam is based on the Tymoshenko beam theory.

$$u_1 = u + z\left[\left(1-\frac{4}{3}\left(\frac{z}{h}\right)^2\right)\phi_1 - \frac{\partial w}{\partial x}\right]$$

$$u_2 = v + z\left[\left(1-\frac{4}{3}\left(\frac{z}{h}\right)^2\right)\phi_2 - \frac{\partial w}{\partial y}\right] \tag{2}$$

where (u_1,u_2,u_3) is the shift corresponding to the coordinate system and is a function of spatial coordinates; (u,v,w) is the shift along the axes x, y, and z, respectively, and ϕ_1 and ϕ_2 are the rotations around the y- and x-axes. All the generalized shifts (u,v,w,ϕ_1,ϕ_2) are functions of (x,y).

Six compatible stretching components of displacement field Equation (2) are

$$\begin{gathered}\varepsilon_1 = \varepsilon_1^{(0)} + z\varepsilon_1^{(1)} + z^3\varepsilon_1^{(3)}, \ \varepsilon_3 = 0, \ \varepsilon_2 = \varepsilon_2^{(0)} + z\varepsilon_2^{(1)} + z^3\varepsilon_2^{(3)}, \\ \varepsilon_4 = \varepsilon_4^{(0)} + z^2\varepsilon_4^{(2)}, \ \varepsilon_5 = \varepsilon_5^{(0)} + z^2\varepsilon_5^{(2)}, \ \varepsilon_6 = \varepsilon_6^{(0)} + z\varepsilon_6^{(1)} + z^3\varepsilon_6^{(3)},\end{gathered} \tag{3}$$

where

$$\varepsilon_1^{(0)} = \frac{\partial u}{\partial x}, \ \varepsilon_2^{(0)} = \frac{\partial v}{\partial x}, \ \varepsilon_4^{(0)} = \phi_2, \ \varepsilon_5^{(0)} = \phi_1, \ \varepsilon_6^{(0)} = \frac{\partial v}{\partial x} + \frac{\partial u}{\partial y},$$

$$\varepsilon_1^{(1)} = \frac{\partial}{\partial x}\left(\phi_1 - \frac{\partial w}{\partial x}\right), \ \varepsilon_2^{(1)} = \frac{\partial}{\partial y}\left(\phi_2 - \frac{\partial w}{\partial y}\right),$$

$$\varepsilon_6^{(1)} = \frac{\partial}{\partial x}\left(\phi_2 - \frac{\partial w}{\partial y}\right) + \frac{\partial}{\partial y}\left(\phi_1 - \frac{\partial w}{\partial x}\right),$$

$$\varepsilon_4^{(2)} = -\frac{4}{h^2}\varepsilon_4^{(0)}, \ \varepsilon_5^{(2)} = -\frac{4}{h^2}\varepsilon_5^{(0)}, \ \varepsilon_1^{(3)} = -\frac{4}{3h^2}\frac{\partial \phi_1}{\partial x},$$

$$\varepsilon_2^{(3)} = -\frac{4}{3h^2}\frac{\partial \phi_2}{\partial y}, \ \varepsilon_6^{(3)} = -\frac{4}{3h^2}\left(\frac{\partial \phi_2}{\partial x} + \frac{\partial \phi_1}{\partial y}\right). \tag{4}$$

The relationships for stretching stresses taking into account the lateral shell deformation coordinates for the kth layer can be expressed as follows:

$$\begin{Bmatrix}\sigma_1\\ \sigma_2\\ \sigma_6\\ \sigma_4\\ \sigma_5\end{Bmatrix}^{(k)} = \begin{bmatrix} c_{11} & c_{12} & 0 & 0 & 0\\ & c_{22} & 0 & 0 & 0\\ & & c_{66} & 0 & 0\\ & & & c_{44} & 0\\ \text{sym.} & & & & c_{55}\end{bmatrix}^{(k)} \begin{Bmatrix}\varepsilon_1\\ \varepsilon_2\\ \varepsilon_6\\ \varepsilon_4\\ \varepsilon_5\end{Bmatrix}, \tag{5}$$

where $c_{ij}^{(k)}$ are the transform elastic modulus depending on the material of each layer,

$$c_{11}^{(k)} = c_{22}^{(k)} = \frac{E_k(z)}{1-\nu_k^2},\quad c_{12}^{(k)} = \frac{\nu_k E_k(z)}{1-\nu_k^2},\quad c_{44}^{(k)} = c_{55}^{(k)} = c_{66}^{(k)} = \frac{E_k(z)}{2(1+\nu_k)}, \tag{6}$$

in which E_k and ν_k are Young's modulus and Poisson's ratio of layer k.

3. Government Equation

The principle of virtual shifting of available problems can be expressed as follows:

$$\int_\Omega \left\{ \int_{-h/2}^{+h/2} \left[\sigma_1^{(k)} \delta\varepsilon_1 + \sigma_5^{(k)} \delta\varepsilon_5 \right] \mathrm{d}z - q\delta w \right\} \mathrm{d}\Omega = 0. \tag{7}$$

or

$$\begin{aligned}\int_\Omega \Big[& N_1 \delta\varepsilon_1^{(0)} + N_2 \delta\varepsilon_2^{(0)} + N_6 \delta\varepsilon_6^{(0)} + M_1 \delta\varepsilon_1^{(1)} + M_2 \delta\varepsilon_2^{(1)} + M_6 \delta\varepsilon_6^{(1)} + Q_4 \delta\varepsilon_4^{(0)} \\ & + Q_5 \delta\varepsilon_5^{(0)} + R_4 \delta\varepsilon_4^{(2)} + R_5 \delta\varepsilon_5^{(2)} + P_1 \delta\varepsilon_1^{(3)} + P_2 \delta\varepsilon_2^{(3)} + P_6 \delta\varepsilon_6^{(3)} \Big] \mathrm{d}\Omega = 0 \end{aligned}, \tag{8}$$

N_i and M_i are the fundamental components of stress resultants and stress couples, P_i are the additional stress couples, and Q_i are resultants of shared stress. They can be expressed as

$$\{N_i, M_i, P_i\} = \sum_{k=1}^{3} \int_{h_{k-1}}^{h_k} \sigma_i^{(k)} \{1, z, z^3\} \mathrm{d}z, (i = 1, 2, 6)$$

$$\{Q_i, R_i\} = \sum_{k=1}^{3} \int_{h_{k-1}}^{h_k} \sigma_i^{(k)} \{1, z^2\} \mathrm{d}z, (i = 4, 5) \tag{9}$$

where h_k and h_{k-1} are the top and bottom *z*-coordinates of the *k*th layer.

The governing equilibrium equations can be derived from the above equation by integrating the displacement gradient in ε_i by parts and setting the coefficients of δu, δv, δw, $\delta\phi_1$ and $\delta\phi_2$ to zero separately. Thus, one obtains

$$\delta u: \frac{\partial N_1}{\partial x} + \frac{\partial N_6}{\partial y} = 0,\quad \delta v: \frac{\partial N_6}{\partial x} + \frac{\partial N_2}{\partial y} = 0,$$

$$\delta w: \frac{\partial^2 M_1}{\partial x^2} + 2\frac{\partial^2 M_6}{\partial x \partial y} + \frac{\partial^2 M_2}{\partial y^2} + q = 0, \tag{10}$$

$$\delta\phi_1: \frac{\partial \hat{P}_1}{\partial x} + \frac{\partial \hat{P}_6}{\partial y} - \hat{Q}_5 = 0,\quad \delta\phi_2: \frac{\partial \hat{P}_6}{\partial x} + \frac{\partial \hat{P}_2}{\partial y} - \hat{Q}_4 = 0,$$

where

$$\hat{P}_i = M_i - \frac{4}{3h^2} P_i,\ (i = 1, 2, 6),$$

$$\hat{Q}_i = Q_i - \frac{4}{h^2} R_i,\ (i = 4,5). \tag{11}$$

Using Equation (5) in Equation (9), the stress resultants can be related to the total strains by

$$N_i = A_{ij}\varepsilon_j^{(0)} + B_{ij}\varepsilon_j^{(1)} + E_{ij}\varepsilon_j^{(3)},\ M_i = B_{ij}\varepsilon_j^{(0)} + D_{ij}\varepsilon_j^{(1)} + F_{ij}\varepsilon_j^{(3)}$$

$$P_i = E_{ij}\varepsilon_j^{(0)} + F_{ij}\varepsilon_j^{(1)} + H_{ij}\varepsilon_j^{(3)},\ (i, j = 1,2,6), \tag{12}$$

$$Q_i = A_{ij}\varepsilon_j^{(0)} + D_{ij}\varepsilon_j^{(2)},\ R_i = D_{ij}\varepsilon_j^{(0)} + F_{ij}\varepsilon_j^{(2)}, (i, j = 4,5)$$

where A_{ij}, B_{ij}, etc., are the non-homogeneous laminate stiff

$$\left\{A_{ij}, B_{ij}, D_{ij}, E_{ij}, F_{ij}, H_{ij}\right\} = \sum_{k=1}^{3}\int_{h_{k-1}}^{h_k} c_{ij}^{(k)}\left\{1, z, z^2, z^3, z^4, z^6\right\}\mathrm{d}z, (i, j = 1,2,6),$$

$$\left\{A_{ii}, D_{ii}, F_{ii}\right\} = \sum_{k=1}^{3}\int_{h_{k-1}}^{h_k} c_{ii}^{(k)}\left\{1, z^2, z^4\right\}\mathrm{d}z, (i = 4,5), \tag{13}$$

and $c_{ij}^{(k)}$ depend on the material properties and orientation of the *k*th non-homogeneous layer.

4. Exact Solutions for Sandwich Beams

Rectangular plates are generally classified following the type of support used. We are here concerned with the exact solution of Equation (10) for a simply supported sandwich plate. The following boundary conditions are imposed at the side edges

$$v = w = \phi_1 = N_1 = M_1 = P_1 = 0 \quad \text{at} \quad x = 0, a,$$

$$u = w = \phi_2 = N_2 = M_2 = P_2 = 0 \quad \text{at} \quad y = 0, b. \tag{14}$$

To solve this problem, Navier presented the external force for the case of sinusoidally distributed load,

$$q(x, y) = q_0 \sin(\lambda x)\sin(\mu y), \tag{15}$$

where $\lambda = \pi/a$, $\mu = \pi/b$ and q_0 represents the intensity of the load at the plate center. Following the Navier solution procedure, we assume the following solution form for $(u, v, w, \phi_1, \phi_2)$ that satisfies the boundary conditions,

$$\begin{Bmatrix} u \\ v \\ w \\ \phi_1 \\ \phi_2 \end{Bmatrix} = \begin{Bmatrix} U\cos(\lambda x)\sin(\mu y) \\ V\sin(\lambda x)\cos(\mu y) \\ W\sin(\lambda x)\sin(\mu y) \\ X\cos(\lambda x)\sin(\mu y) \\ Y\sin(\lambda x)\cos(\mu y) \end{Bmatrix} \tag{16}$$

where U, V, W, X, and Y are arbitrary parameters to be determined. Substituting from Equation (16) into Equation (10), we obtain

$$[C]\{\Delta\} = \{F\}, \tag{17}$$

where $\{\Delta\}$ and $\{F\}$ denote the columns

$$\{\Delta\}^t = \{U, V, W, X, Y\},\ \{F\}^t = \{0, 0, -q_0, 0, 0\}. \tag{18}$$

The elements $C_{ij} = C_{ji}$ of the coefficient matrix $[C]$ are given by

$$C_{11} = -\lambda^2 A_{11} - \mu^2 A_{66}, \quad C_{12} = -\lambda\mu\left(A_{12} + A_{66}\right),$$
$$C_{13} = \lambda\left[\lambda^2 B_{11} + \left(B_{12} + 2B_{66}\right)\mu^2\right],$$
$$C_{14} = -\lambda^2 B_{11} - \mu^2 B_{66} + \frac{4}{3h^2}\left(\lambda^2 E_{11} + \mu^2 E_{66}\right),$$
$$C_{15} = -\lambda\mu\left(B_{12} + B_{66}\right) + \frac{4}{3h^2}\lambda\mu\left(E_{11} + E_{66}\right), \tag{19}$$
$$C_{22} = -\lambda^2 A_{66} - \mu^2 A_{22}, \; C_{23} = \mu\left[\left(B_{12} + 2B_{66}\right)\lambda^2 + B_{22}\mu^2\right],$$
$$C_{24} = C_{15}, \; C_{25} = -\lambda^2 B_{66} - \mu^2 B_{22} + \frac{4}{3h^2}\left(\lambda^2 E_{66} + \mu^2 E_{22}\right),$$
$$C_{33} = -\lambda^4 D_{11} - 2\left(D_{12} + 2D_{66}\right)\lambda^2\mu^2 - \mu^4 D_{22},$$
$$C_{34} = -\lambda\left[\lambda^2 D_{11} + \left(D_{12} + 2D_{66}\right)\mu^2\right] - \frac{4}{3h^2}\lambda\left[\lambda^2 F_{11} + \left(F_{12} + 2F_{66}\right)\mu^2\right],$$
$$C_{35} = -\mu\left[\mu^2 D_{22} + \left(D_{12} + 2D_{66}\right)\lambda^2\right] - \frac{4}{3h^2}\mu\left[\mu^2 F_{22} + \left(F_{12} + 2F_{66}\right)\lambda^2\right],$$
$$C_{44} = -\lambda^2 D_{11} - \mu^2 D_{66} - A_{55} - \frac{16}{9h^4}\left(\lambda^2 H_{11} + \mu^2 H_{66}\right) + \frac{8}{3h^2}\left(3D_{55} + \lambda^2 F_{11} + \mu^2 F_{66} - \frac{6}{h^2}F_{55}\right),$$
$$C_{45} = -\lambda\mu\left(D_{12} + D_{66}\right) + \frac{8}{3h^2}\lambda\mu\left(F_{12} + F_{66}\right) - \frac{16}{9h^2}\lambda\mu\left(H_{12} + H_{66}\right),$$
$$C_{55} = -\lambda^2 D_{66} - \mu^2 D_{22} - A_{44} - \frac{16}{9h^4}\left(\lambda^2 H_{66} + \mu^2 H_{22}\right) + \frac{8}{3h^2}\left(3D_{44} + \lambda^2 F_{66} + \mu^2 F_{22} - \frac{6}{h^2}F_{44}\right).$$

Additionally, the formula will be replaced Equation (16) into Equation (4), Can we get the voltage components related to Young's modulus and the arbitrary parameters U, V, W, X, and Y as follows:

$$\sigma_1^{(k)} = -\frac{E_k(z)}{1-\nu_k^2}\left\{\lambda U + \nu_k\mu V - z\left(\lambda^2 + \nu_k\mu^2\right)W + z\left(1 - \frac{4}{3h^2}z^2\right)\left(\lambda X + \nu_k\mu Y\right)\right\}\sin(\lambda x)\sin(\mu y),$$
$$\sigma_2^{(k)} = -\frac{E_k(z)}{1-\nu_k^2}\left\{\nu_k\lambda U + \mu V - z\left(\nu_k\lambda^2 + \mu^2\right)W + z\left(1 - \frac{4}{3h^2}z^2\right)\left(\nu_k\lambda X + \mu Y\right)\right\}\sin(\lambda x)\sin(\mu y),$$
$$\sigma_4^{(k)} = \frac{E_k(z)}{2\left(1+\nu_k\right)}\left(1 - \frac{4}{h^2}z^2\right)Y\sin(\lambda x)\cos(\mu y), \tag{20}$$
$$\sigma_5^{(k)} = \frac{E_k(z)}{2\left(1+\nu_k\right)}\left(1 - \frac{4}{h^2}z^2\right)X\cos(\lambda x)\sin(\mu y),$$

$$\sigma_6^{(k)} = \frac{E_k(z)}{2(1+\nu_k)}\left\{\mu U + \lambda V - 2z\lambda\mu W + z\left(1-\frac{4}{3h^2}z^2\right)(\mu X + \lambda Y)\right\}\cos(\lambda x)\cos(\mu y).$$

5. Viscoelastic Solution

5.1. The (e-v-e) Sandwich Plate

In this issue, the core of the sandwich plate as an isotropic viscoelastic is made of an isotropic viscoelastic material with the same elastic properties, i.e. $E_1 = E_3 = E$ and $\nu_1 = \nu_3 = \nu$. Note that a viscoelastic modulus of the core layer is given

$$E_2 = \frac{9K\varpi}{2+\varpi}, \tag{21}$$

K is volumetric compression (mass module) and is assumed unrelaxed. In other words, K = constant and ϖ is dimensionless kernel of the relaxation function, which are related to the corresponding Poisson's ratio of the core according to the equation.

$$\nu_2 = \frac{1-\varpi}{2+\varpi}. \tag{22}$$

5.2. The (v-e-v) Sandwich Plate

Here, the core of the sandwich plate is used as an isotropic elastic material, but the surface is made of viscoelastic material with the same viscoelastic properties. $E_2 = E$ and $\nu_2 = \nu$. The viscoelastic properties of the two faces are given by

$$E_1 = E_3 = \frac{9K\varpi}{2+\varpi},\ \ \nu_1 = \nu_3 = \frac{1-\varpi}{2+\varpi}. \tag{23}$$

To solve the quasi-static problem of the linear theory of viscoelastic composites, this method can be used to reduce the non-homogeneous isotropic viscoelastic problems to a sequence of continuous anisotropy, as is done in the elastic case (see [40] [41]). Get it with Equations (21), (22), and (23) into Equation (20)

$$\sigma_{ij}^{(k)} = F_{ij}^{(k)}(\varpi)q_0(t),\ i=1,2,4,5,6,\ j=1,2,\ k=1,2,3, \tag{24}$$

However, $q_0(t)$ is a temporary function that performs a viscoelastic response to a bending problem. According to Il'yushin's approximation method [40], the function $F_{ij}^{(k)}$ can be displayed in the form

$$F_{ij}^{(k)}(\varpi) = \sum_{l=1}^{5} A_{ijl}^{(k)}\Phi(\varpi), \tag{25}$$

where $\Phi(\varpi)$ are some known kernels, constructed based on the kernel ϖ and may chosen in the form

$$\Phi_1 = 1, \Phi_2 = \varpi, \Phi_3 = \bar{\Pi} = \frac{1}{\varpi}, \Phi_4 = \bar{g}_{\beta_1}, \Phi_5 = \bar{g}_{\beta_2}, \tag{26}$$

where $\bar{g}_{\beta_m} = \frac{1}{1+\beta_m\varpi}$, $m = 1,2$. The coefficients $A_{ijl}^{(k)}$ are determined by the system of algebraic equations

$$\sum_{l=1}^{5} L_{ij} A_{ijl}^{(k)} = B_{ijl}^{(k)}, \tag{27}$$

where

$$L_{ij} = \int_0^1 \Phi_i(\varpi)\Phi_j(\varpi)\,\mathrm{d}\varpi, \quad B_{ijl}^{(k)} = \int_0^1 \Phi_i(\varpi) F_{ijl}^{(k)}(\varpi)\,\mathrm{d}\varpi. \tag{28}$$

The viscoelastic solution may now record to obtain explicit formulae for stresses $\sigma_{ij}^{(k)}$ as functions of the time t. Then,

$$\begin{aligned}\sigma_{ij}^{(k)} &= A_{ij1}^{(k)} q_0(t) + A_{ij2}^{(k)} \int_0^1 \omega(t-\tau)\,\mathrm{d}q_0(t) + A_{ij3}^{(k)} \int_0^1 \pi(t-\tau)\,\mathrm{d}q_0(t) \\ &\quad + A_{ij4}^{(k)} \int_0^1 g_{\beta_1}(t-\tau)\,\mathrm{d}q_0(t) + A_{ij5}^{(k)} \int_0^1 g_{\beta 2}(t-\tau)\,\mathrm{d}q_0(t).\end{aligned} \tag{29}$$

Taking $q(t) = q_0 H(t)$, where $H(t)$ is the Heaviside's unit step function

$$H(t) = \begin{cases} 1 & \text{if } t \ge 0, \\ 0 & \text{if } t < 0, \end{cases} \tag{30}$$

the above formulae for two problems take the form

$$\sigma_{ij}^{(k)}(\varpi) = \overline{q}_0 \left[A_{ij1}^{(k)} H(t) + A_{ij2}^{(k)} \omega(\tau) + \pi(\tau) + A_{ij4}^{(k)} g_{\beta_1}(\tau) + A_{ij5}^{(k)} g_{\beta_2}(\tau) \right], \tag{31}$$

where $\omega(t) = \varpi, \pi(t) = \overline{\Pi}$ and $g_{\beta_m}(t) = \overline{g}_{\beta_m}, (m = 1, 2)$.

Assuming an exponential relaxation function

$$\omega(t) = c_1 + c_2 \mathrm{e}^{-\alpha t}, \quad \alpha = \frac{1}{t_s} \tag{32}$$

where c_1, c_2 are constants that to be determined, and t_s is the relaxation time. The function $\pi(t), g_{\beta_m}(t), (m = 1, 2)$. This can be determined by deducing the Laplace-Carson transform of these functions. Transformation of known Laplace-Carson function $\omega(t)$, specified in Appendix A.

$$\pi(t) = \frac{1}{c_1}\left[1 - \frac{c_2}{c_1 + c_2} \mathrm{e}^{-\frac{c_1 \alpha t}{c_1 + c_2}}\right], \quad \tau = \alpha t, \tag{33}$$

$$g_{\beta_m}(t) = \frac{1}{1 + c_1 \beta_m}\left[1 - \frac{c_2 \beta_m}{1 + (c_1 + c_2)\beta_m} \mathrm{e}^{\frac{-(1 + c_1 \beta_m)\tau}{1 + (c_1 + c_2)\beta_m}}\right]. \tag{34}$$

Therefore, the final shape of the bending stresses load concerning the time parameter τ

$$\begin{aligned}\Sigma_{ij}^{(k)} &= A_{ij1}^{(k)} H(t) + A_{ij2}^{(k)} \left[c_1 + c_2 \mathrm{e}^{-\alpha t}\right] + \frac{A_{ij3}^{(k)}}{c_1}\left[1 - \frac{c_2}{c_1 + c_2} \mathrm{e}^{-\frac{c_1 \alpha t}{c_1 + c_2}}\right] \\ &\quad + \frac{A_{ij4}^{(k)}}{1 + c_1 \beta_1}\left[1 - \frac{c_2 \beta_1}{1 + (c_1 + c_2)\beta_1} \mathrm{e}^{\frac{-(1 + c_1 \beta_1)\tau}{1 + (c_1 + c_2)\beta_1}}\right] \\ &\quad + \frac{A_{ij5}^{(k)}}{1 + c_1 \beta_2}\left[1 - \frac{c_2 \beta_2}{1 + (c_1 + c_2)\beta_2} \mathrm{e}^{\frac{-(1 + c_1 \beta_2)\tau}{1 + (c_1 + c_2)\beta_2}}\right],\end{aligned} \tag{35}$$

where $\Sigma_{ij}^{(k)} = \sigma_{ij}^{(k)} / \overline{q}_0$.

6. Various Types of Sandwich Plates

6.1. (1-2-1) Sandwich Plate

Here, the t

$$h_1 = -h/4, h_2 = h/4. \tag{36}$$

6.2. (1-1-1) Sandwich Plate

The plate consists of three layers of the same thickness. So, one takes

$$h_1 = -h/6, h_2 = h/6. \tag{37}$$

6.3. (2-1-2) Sandwich Plate

In this case, the core thickness is half the thickness of the face. It shows it

$$h_1 = -h/10, h_2 = h/10. \tag{38}$$

6.4. (1-0-1) Sandwich Plate

In this case, there is no core layer, and made of only two equal-thickness layers, i.e. Thus,

$$h_1 = h_2 = 0. \tag{39}$$

7. Numerical Results and Discussion

The simple supported numerical results on sandwich plates are achieved. The relaxation time α is still unknown, and the time parameter $\tau = -\alpha t$ is given about it. Poisson's ratio for the elastic plate is taken for a value of 0.25, with $\zeta = E/K$ being a constitutive parameter. Unless otherwise stated, this is assumed to be accepted

$$b/a = 0.5, \quad \zeta = 0.1, \quad a/h = 5, \quad c_1 = 0.1, \quad c_2 = 0.9. \tag{40}$$

The following nondimensional response characteristics are used throughout the calculations:

$$\sigma_1 = \Sigma_1\left(\frac{a}{2},\frac{b}{2},\bar{z}\right), \quad \sigma_2 = \Sigma_2\left(\frac{a}{2},\frac{b}{2},\bar{z}\right), \quad \sigma_6 = \Sigma_6\left(0,0,\bar{z}\right),$$

$$\sigma_4 = \Sigma_4\left(\frac{a}{2},0,\bar{z}\right), \quad \sigma_5 = \Sigma_5\left(0,\frac{b}{2},\bar{z}\right), \quad w = \frac{K}{h\bar{q}_0} w\left(\frac{a}{2},\frac{b}{2}\right). \tag{41}$$

in which $\bar{z} = z/h$.

Tables 1-3 include the stresses and bending deflection of two uneven viscoelastic (e-v-e) and (v-e-v) sandwich panels. The influence of constitutive parameters ζ, from thickness a/h and aspect ratio b/a is shown. The results obtained with the current theory are compared with those in Ref. [42]. As shown in Table 1, the stresses σ_1, $|\sigma_6|$, σ_4 and deflection w increase with the increasing of side-to-thickness ratio a/h for both cases (e-v-e) and (v-e-v). The stresses σ_1,

$|\sigma_6|$, and deflection w increases with the increasing aspect ratio b/a for the two cases (e-v-e) and (v-e-v), as shown in Table 2. However, the shear stress σ_4 is decreasing with the increase in the aspect ratio b/a for the two cases. The deflection w is rapidly increasing with the increase in both a/h and b/a ratios for both cases. Table 3 follows as the constitutive parameters increase. The stresses in the first (e-v-e) case (viscoelastic core) are reduced and increase in the second (v-e-v) case (elastic core) case. The deflection w is decreasing with increasing constitutive parameters ζ for both cases.

Table 1. Non-dimensionless deflection and stresses vs different values of side-to-thickness ratio a/h for both (e-v-e) and (v-e-v) sandwich plates ($\bar{z}=1/12$, $\omega=0.1$, $b/a=0.5$, and $\zeta=0.1$).

a/h	σ_1		σ_4		σ_6		w	
	Ref. [42]	Present	Ref. [42]	Present	Ref. [42]	Present	Ref. [42]	Present
e-v-e								
5	1.816	1.762	1.012	1.100	−0.765	−0.742	29.243	28.634
10	7.264	7.210	2.023	2.206	−3.059	−3.036	391.838	389.478
15	16.343	16.289	3.034	3.311	−6.882	−6.859	1912.391	1907.112
20	29.054	29.000	4.045	4.416	−12.234	−12.211	5965.244	5955.878
25	45.397	45.343	5.056	5.520	−19.115	−19.092	14474.470	14459.850
v-e-v								
5	0.137	0.127	0.177	0.316	−0.103	−0.095	10.937	12.782
10	0.546	0.535	0.353	0.639	−0.409	−0.402	125.321	132.956
15	1.227	1.216	0.529	0.960	−0.920	−0.912	587.874	605.160
20	2.181	2.170	0.705	1.281	−1.636	−1.628	1806.463	1837.260
25	3.407	3.397	0.881	1.602	−2.555	−2.548	4352.104	4400.273

Table 2. Non-dimensionless deflection and stresses vs different values of aspect ratio b/a for both (e-v-e) and (v-e-v) sandwich plates ($\bar{z}=1/12$, $\omega=0.1$, $a/h=5$, and $\zeta=0.1$).

b/a	σ_1		σ_4		σ_6		w	
	Ref. [42]	Present	Ref. [42]	Present	Ref. [42]	Present	Ref. [42]	Present
e-v-e								
0.5	1.816	1.762	1.012	1.100	−0.765	−0.742	29.243	28.634
1.0	5.974	5.903	1.264	1.378	−2.390	−2.361	159.003	157.518
1.5	9.543	9.461	1.167	1.273	−3.054	−3.028	296.397	294.351
2.0	11.851	11.763	1.012	1.103	−3.059	−3.036	391.838	389.478

Continued

				v-e-v				
0.5	0.137	0.127	0.177	0.316	−0.103	−0.095	10.937	12.782
1.0	0.533	0.517	0.221	0.399	−0.320	−0.310	52.834	57.574
1.5	0.908	0.888	0.204	0.369	−0.409	−0.400	95.781	102.376
2.0	1.159	1.137	0.177	0.320	−0.409	−0.402	125.321	132.956

Table 3. Non-dimensionless deflection and stresses vs different values of constitutive parameter ζ for both (e-v-e) and (v-e-v) sandwich plates ($\bar{z} = 1/12$, $\omega = 0.1$, $b/a = 0.5$, and $a/h = 5$).

a/h	σ_1		σ_4		σ_6		w	
	Ref. [42]	Present	Ref. [42]	Present	Ref. [42]	Present	Ref. [42]	Present
				e-v-e				
0.1	1.816	1.762	1.012	1.100	−0.765	−0.742	29.243	28.634
0.3	0.964	0.921	0.586	0.792	−0.406	−0.388	12.939	13.307
0.5	0.681	0.647	0.413	0.623	−0.287	−0.273	8.532	9.109
1.0	0.400	0.377	0.237	0.407	−0.169	−0.159	4.666	5.239
1.5	0.284	0.267	0.167	0.303	−0.120	−0.113	3.222	3.707
2.0	0.220	0.207	0.129	0.241	−0.093	−0.087	2.462	2.874
5.0	0.094	0.088	0.054	0.108	−0.040	−0.037	1.021	1.229
10.0	0.049	0.045	0.028	0.057	−0.021	−0.019	0.518	0.630
				v-e-v				
0.1	0.137	0.127	0.177	0.316	−0.103	−0.095	10.937	12.782
0.3	0.350	0.330	0.433	0.641	−0.263	−0.247	9.735	10.402
0.5	0.514	0.489	0.610	0.807	−0.385	−0.367	8.886	9.094
1.0	0.812	0.782	0.882	1.006	−0.609	−0.586	7.54	7.399
1.5	1.03	0.998	1.035	1.1	−0.773	−0.749	6.729	6.525
2.0	1.208	1.175	1.134	1.156	−0.906	−0.882	6.171	5.963
5.0	1.939	1.907	1.368	1.297	−1.454	−1.431	4.538	4.415
10.0	2.682	2.654	1.47	1.382	−2.011	−1.991	3.411	3.352

The variations in plate thickness and time parameter τ for various types of non-uniform viscoelastic sandwich plates are shown in **Figures 2-11**. The results obtained for various values of side-to-thickness ratio a/h, aspect ratio b/a, and constitutive parameter ζ in two cases (a) (e-v-e) and (b) (v-e-v).

Figure 2 and Figure 3 illustrate the transverse shear stresses σ_4 and σ_5 vs several types of thickness of the two cases. The dimensionless stresses take greater values in the core (viscoelastic) in the first case (e-v-e) and vice versa in the second case (v-e-v). Also note that in the first case, the stresses increase with reduced core thickness compared to other surface thicknesses, while for the other case, it decreases. Without a core, this means that the plate is completely elastic in the first case and completely viscoelastic in the second case. The stresses have the same curve-related shape.

Figure 4 shows the dimensionless stress σ_1 versus the time parameter τ at various values of $\bar{z}$ for the two cases of (1-1-1) sandwich plates. The variation of σ_1 for the two cases at different layers is clearly shown as a variation of the time parameter τ and is constant at $\tau > 12$. Figure 5 and Figure 6 show the tangential stress σ_6 and bending deflection w for the time parameter τ for the two cases of the sandwich plates at the core layer ($\bar{z} = 1/12$), for different types: (1-1-1), (2-1-2), and (1-2-1) sandwich plates. The tangential stress of the (e-v-e) plate increases as core thickness increases compared to the thickness of the face (upper and lower) layers. In this case, σ_6 increasing with increasing time parameter and receiving high and fixed values for a larger time. However, the tangential stress of the (v-e-v) plate increases with the decrease in the core thickness compared with the thickness of the face (upper and lower) layers. Also, σ_6 is very sensitive to the variation of time parameter. It is no longer decreasing to get its local minimum value, then it is no longer increasing to get its local maximum value then it is decreasing again to get its low and fixed value for a larger time. For both (e-v-e) and (v-e-v) cases, the (1-1-1) sandwich plate yields the largest deflection, while the (1-2-1) sandwich plate yields the smallest deflection. Also, the deflection w is very sensitive to the variation of the time parameter for the second case.

Figure 7 and Figure 8 show variations of dimensionless stress σ_1 and the deflection w for the time parameter τ at the core ($\bar{z} = 1/12$) and different values of a/h. It should be noted that as the ratio of thickness ratio a/h dimensionless stress and deflection increase. However, the (e-v-e) plate provides the maximum stress and deflection compared with the (v-e-v) plates.

Figure 9 shows the variations of dimensionless shear stress σ_4 compared to the time parameter τ at the core ($\bar{z} = 1/12$) with different aspect ratios b/a in the two cases. The shear stress increases with increasing aspect b/a, and it is very sensitive to variation of the time parameter. The (e-v-e) plate provides the maximum shear voltage compared to the(v-e-v) plates.

Finally, Figure 10 and Figure 11 show variations of dimensionless stress σ_1 and deflection w versus the time parameter τ at the core ($\bar{z} = 1/12$) with different values of the constitutive parameter ζ. Stress increases with reduced constitutive parameter ζ for the (e-v-e) plate, and vice versa for the other plate. However, in two cases the dimensionless deflection increases as ζ decreases.

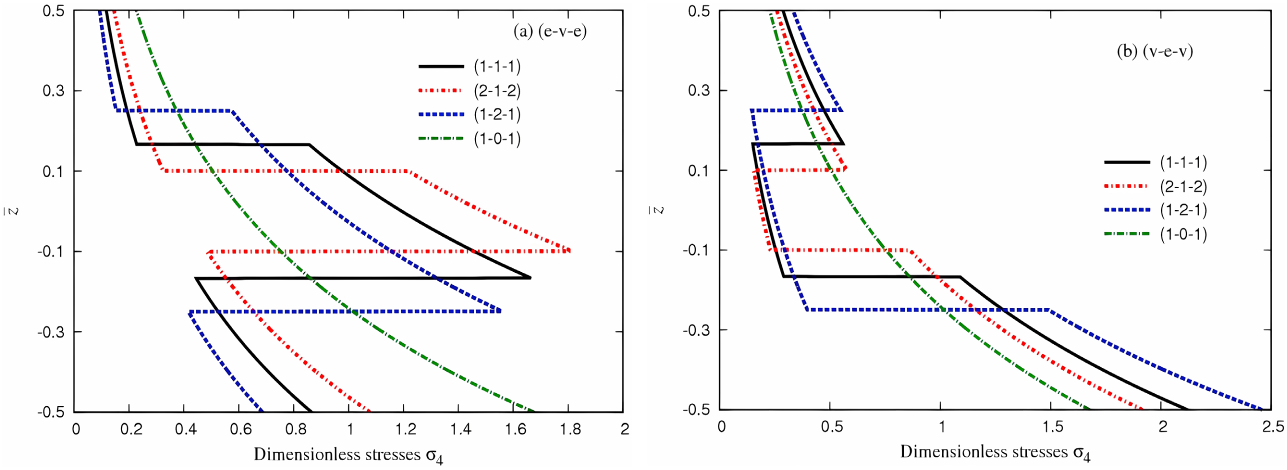

Figure 2. Transverse shear stress σ_4 through the plate thickness for different types of sandwich plates of two cases (e-v-e) and (v-e-v).

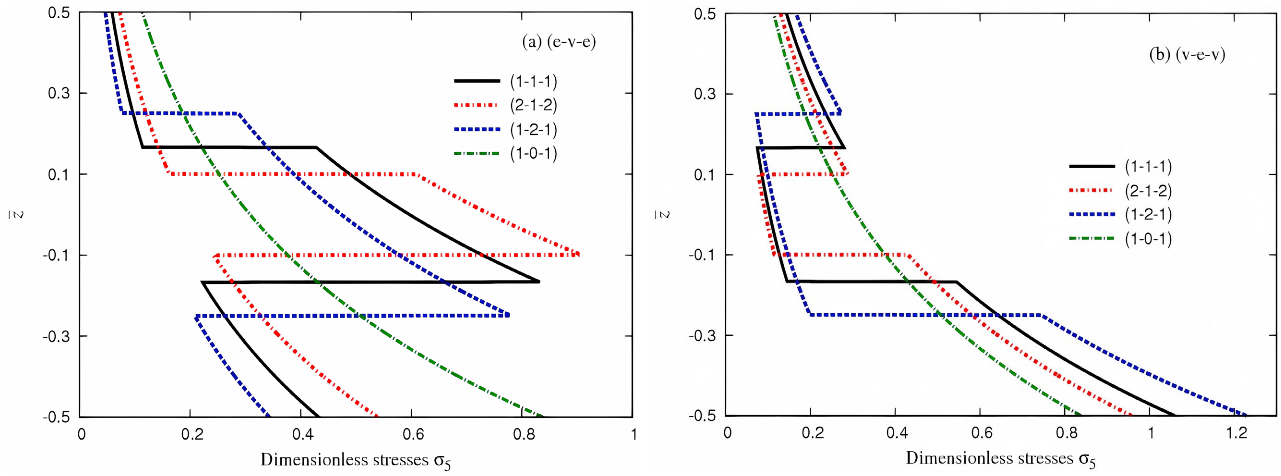

Figure 3. Transverse shear stress σ_5 through the plate thickness for different types of sandwich plates of two cases (e-v-e) and (v-e-v.

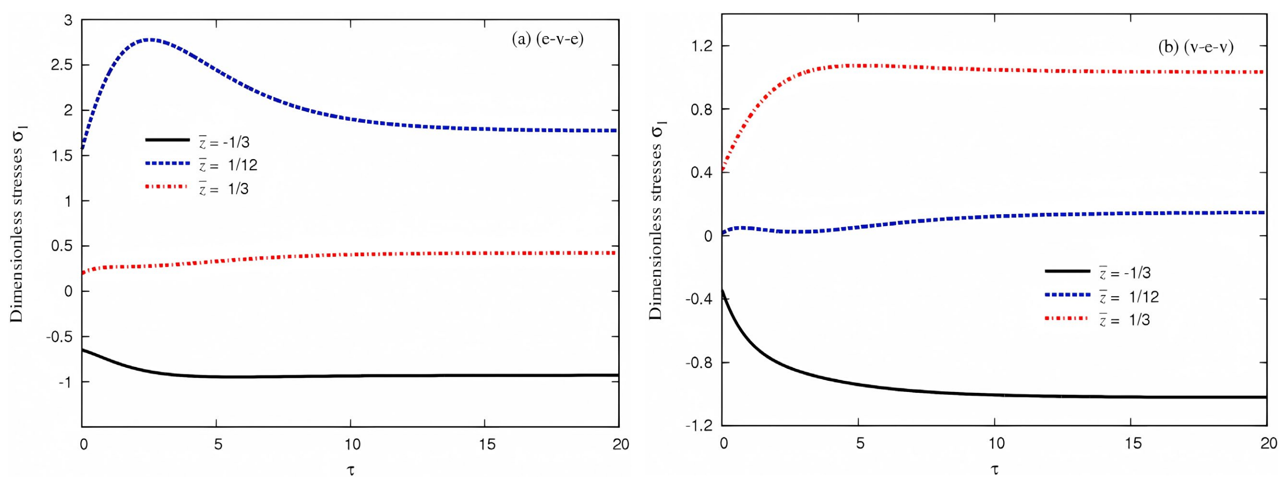

Figure 4. Dimensionless stresses σ_1 compared to time parameter τ at different values of the thickness $\bar{z}$ for (1-1-1) sandwich plates of two cases (e-v-e) and (v-e-v).

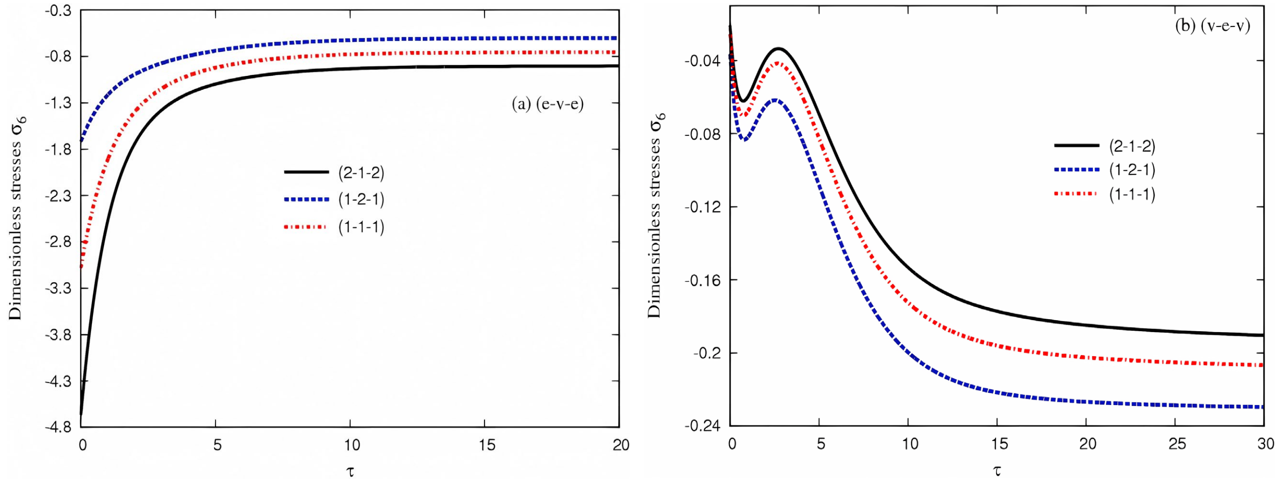

Figure 5. Dimensionless stresses σ_6 compared to time parameter τ at different types of sandwich plates of two cases (e-v-e) and (v-e-v).

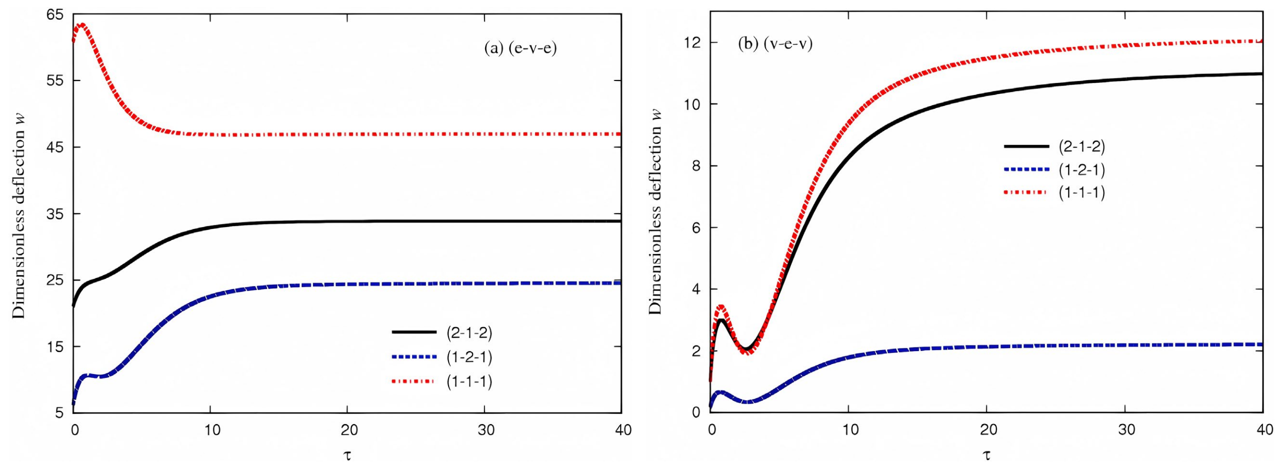

Figure 6. Dimensionless deflection w compared to time parameter τ at different types of sandwich plates of two cases (e-v-e) and (v-e-v).

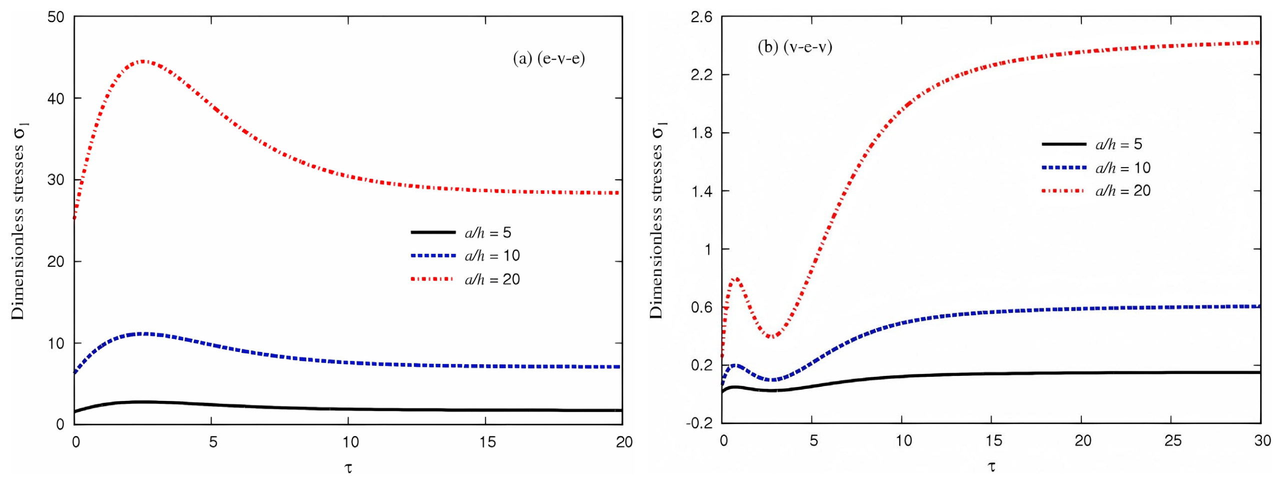

Figure 7. Dimensionless stresses σ_1 compared to time parameter τ with different values of side-to-thickness a/h for (1-1-1) sandwich plates of two cases (e-v-e) and (v-e-v).

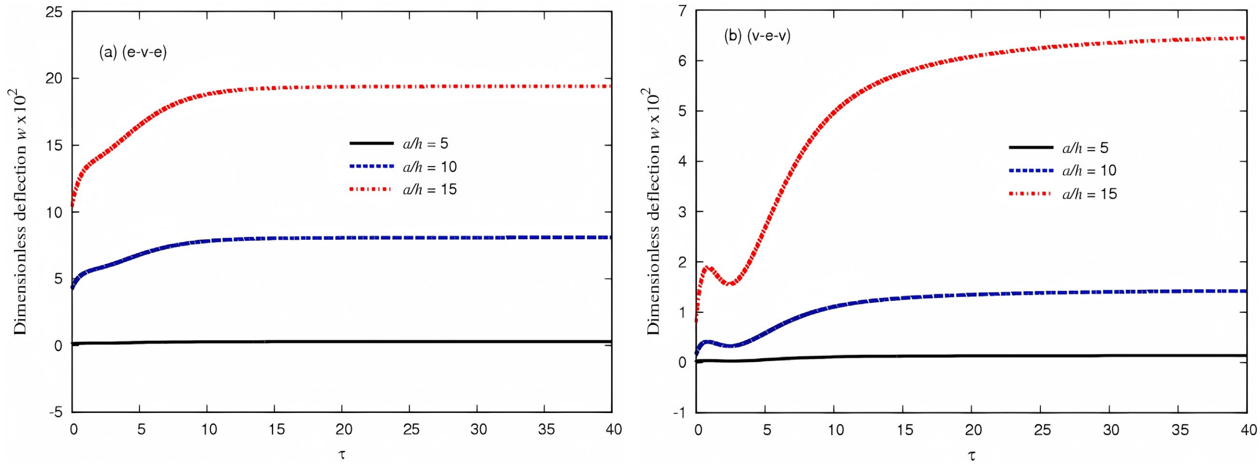

Figure 8. Dimensionless deflection w compared to time parameter τ with different values of side-to-thickness a/h for (1-1-1) sandwich plates of two cases (e-v-e) and (v-e-v).

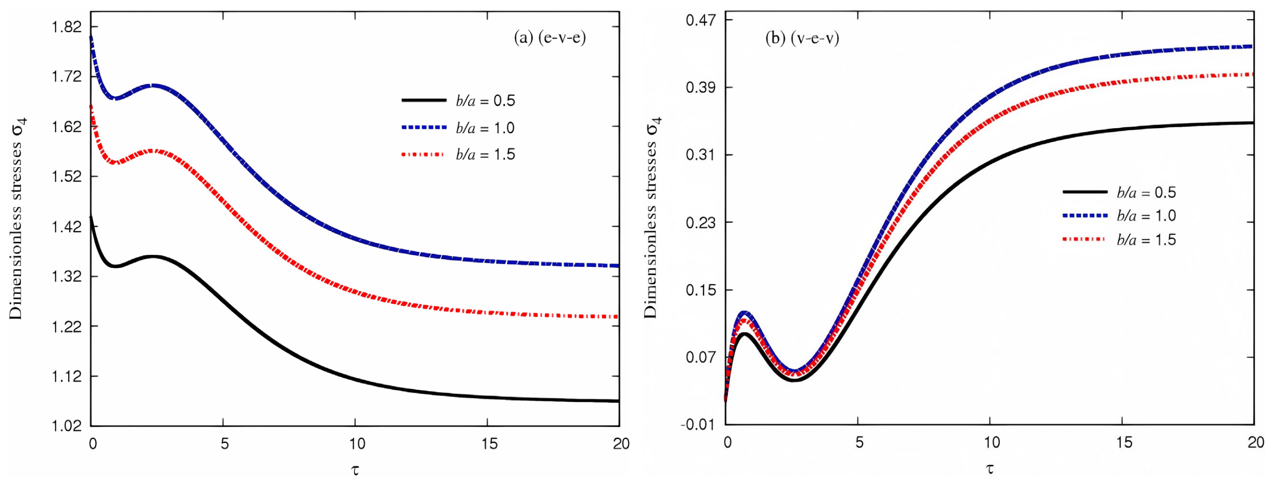

Figure 9. Dimensionless stresses σ_4 compared to time parameter τ with different values of aspect ratio b/a for (1-1-1) sandwich plates of two cases (e-v-e) and (v-e-v).

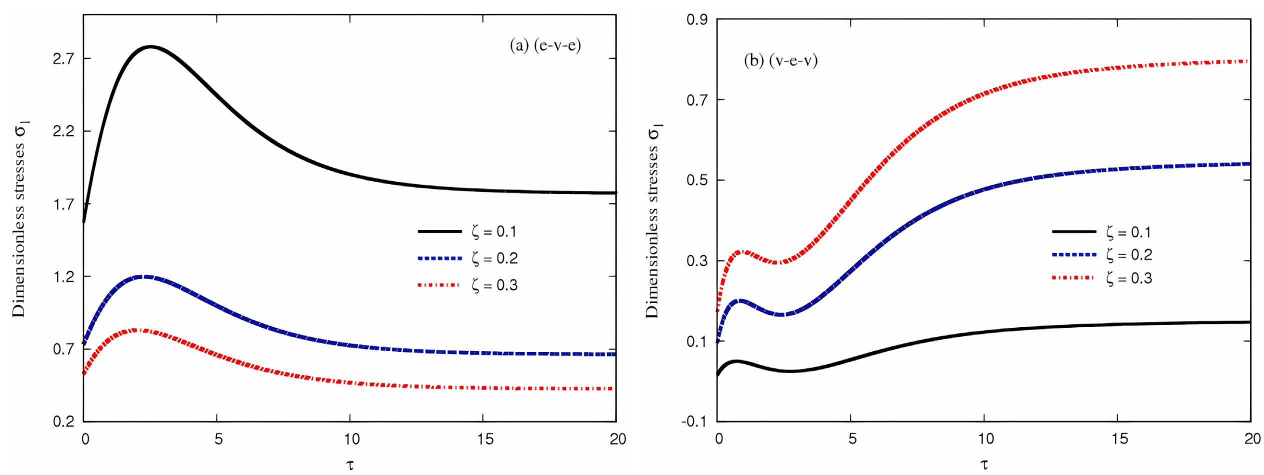

Figure 10. Dimensionless stresses σ_1 compared to time parameter τ with different values of constitutive parameter ζ for (1-1-1) sandwich plates of two cases (e-v-e) and (v-e-v).

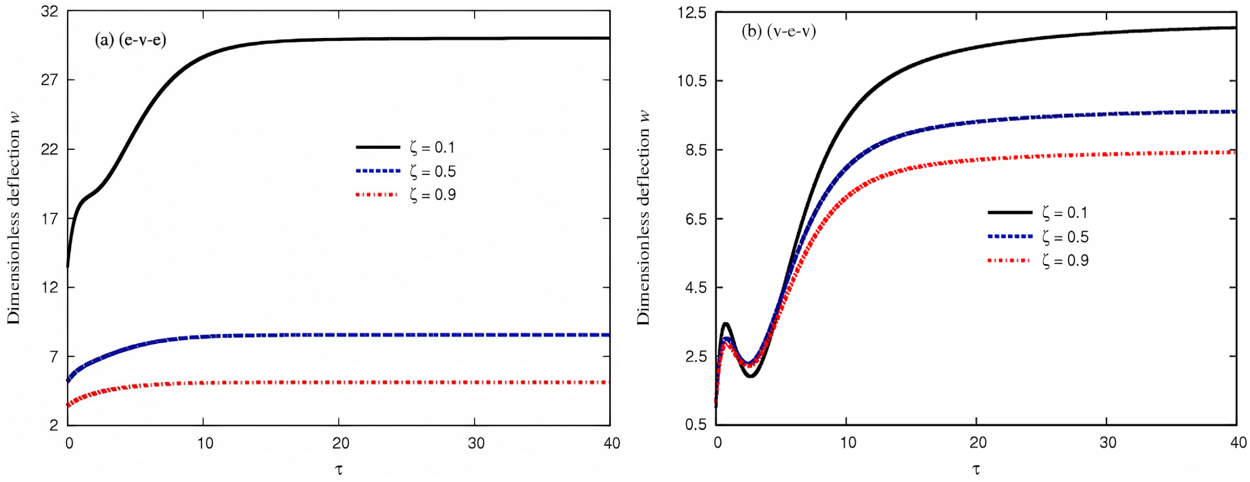

Figure 11. Dimensionless deflection compared to time parameter τ with different values of constitutive parameter ζ for (1–1–1) sandwich plates of two cases (e-v-e) and (v-e-v).

8. Conclusion

A refined, higher-order plate theory has been developed for the bending response of non-homogenous viscoelastic sandwich plates. The current theory includes the same dependent unknowns as first-order shear deformation theory [42] but considers that no transverse shear correction factors are needed because a correct representation of the transverse shear strain is given. Numerical results for stresses and deflections were presented for the quasi-static analysis of heterogeneous viscoelastic sandwich plates exposed to sinusoidal loads. Numerical calculations include side-to-thickness a/h, constitutive parameter ς, and aspect ratio b/a, at time parameter τ on deflections and stress show how the dimensionless stresses and deflection depend on the elastic properties of the layers i.e., both face layers are elastic or viscoelastic. Furthermore, dimensionless stresses and deflection variation compared to time parameters have high sensitivity to the viscoelastic face layers or core layer.

Conflicts of Interest

The authors declare no conflicts of interest regarding the publication of this paper.

References

[1] Hildebrand, F.B., Reissner, E. and Thomas, G.B. (1949) Note on the Foundations of the Theory of Small Displacements of Orthotropic Shells. *Technical Notes National Advisory Committee for Aeronautics*, No. 1833, 59. https://mathscinet.ams.org/mathscinet/relay-station?mr=0030886

[2] Nelson, R.B. and Lorch, D.R. (1974) A Refined Theory for Laminated Orthotropic Plates. *Journal of Applied Mechanics*, **41**, 177-183. https://doi.org/10.1115/1.3423219

[3] Librescu, L. (1975) Elastostatics and Kinetics of Anisotropic and Heterogeneous Shell-Type Structures. Springer. https://link.springer.com/book/9789028600355

[4] Lo, K.H., Christensen, R.M. and Wu, E.M. (1977) A High-Order Theory of Plate Deformation—Part 1: Homogeneous Plates. *Journal of Applied Mechanics*, **44**, 663-668.

https://doi.org/10.1115/1.3424154

[5] Lo, K.H., Christensen, R.M. and Wu, E.M. (1977) A High-Order Theory of Plate Deformation—Part 2: Laminated Plates. *Journal of Applied Mechanics*, **44**, 669-676. https://doi.org/10.1115/1.3424155

[6] Murthy, M.V. (1981) An Improved Transverse Shear Deformation Theory for Laminated Anisotropic Plates. National Technical Information Service. https://search.worldcat.org/title/9086056

[7] Reddy, J.N. (1984) A Simple Higher-Order Theory for Laminated Composite Plates. *Journal of Applied Mechanics*, **51**, 745-752. https://doi.org/10.1115/1.3167719

[8] Reddy, J.N. and Liu, C.F. (1985) A Higher-Order Shear Deformation Theory of Laminated Elastic Shells. *International Journal of Engineering Science*, **23**, 319-330. https://doi.org/10.1016/0020-7225(85)90051-5

[9] Reddy, J.N., Barbero, E.J. and Teply, J.L. (1989) A Plate Bending Element Based on a Generalized Laminate Plate Theory. *International Journal for Numerical Methods in Engineering*, **28**, 2275-2292. https://doi.org/10.1002/nme.1620281006

[10] Reddy, J.N. and Khdeir, A.A. (1989) Buckling and Vibration of Laminated Composite Plates Using Various Plate Theories. *AIAA Journal*, **27**, 1808-1817. https://doi.org/10.2514/3.10338

[11] Zenkour, A.M. (2005) A Comprehensive Analysis of Functionally Graded Sandwich Plates: Part 1—Deflection and Stresses. *International Journal of Solids and Structures*, **42**, 5224-5242. https://doi.org/10.1016/j.ijsolstr.2005.02.015

[12] Zenkour, A.M. (2005) A Comprehensive Analysis of Functionally Graded Sandwich Plates: Part 2—Buckling and Free Vibration. *International Journal of Solids and Structures*, **42**, 5243-5258. https://doi.org/10.1016/j.ijsolstr.2005.02.016

[13] Whitney, J.M. and Pagano, N.J. (1970) Shear Deformation in Heterogeneous Anisotropic Plates. *Journal of Applied Mechanics*, **37**, 1031-1036. https://doi.org/10.1115/1.3408654

[14] Bert, C.W. (1973) Simplified Analysis of Static Shear Factors for Beams of Nonhomogeneous Cross Section. *Journal of Composite Materials*, **7**, 525-529. https://doi.org/10.1177/002199837300700410

[15] Reissner, E. (1991) A Mixed Variational Equation for a Twelfth-Order Theory of Bending of Nonhomogeneous Transversely Isotropic Plates. *Computational Mechanics*, **7**, 355-360. https://doi.org/10.1007/bf00350164

[16] Reissner, E. (1994) On the Equations of an Eighth-Order Theory for Nonhomogeneous Transversely Isotropic Plates. *International Journal of Solids and Structures*, **31**, 89-96. https://doi.org/10.1016/0020-7683(94)90177-5

[17] Fares, M.E. and Zenkour, A.M. (1999) Buckling and Free Vibration of Non-Homogeneous Composite Cross-Ply Laminated Plates with Various Plate Theories. *Composite Structures*, **44**, 279-287. https://doi.org/10.1016/s0263-8223(98)00135-4

[18] Zenkour, A.M. and Fares, M.E. (1999) Non-Homogeneous Response of Cross-Ply Laminated Elastic Plates Using a Higher-Order Theory. *Composite Structures*, **44**, 297-305. https://doi.org/10.1016/s0263-8223(99)00006-9

[19] Zenkour, A.M. and Radwan, A.F. (2020) Bending and Buckling Analysis of FGM Plates Resting on Elastic Foundations in Hygrothermal Environment. *Archives of Civil and Mechanical Engineering*, **20**, Article No. 112. https://doi.org/10.1007/s43452-020-00116-z

[20] Ellali, M. Bouazza, M. and Zenkour, A.M. (2023) Wave Propagation of FGM Plate via New Integral Inverse Cotangential Shear Model with Temperature-Dependent

Material Properties. *Geomechanics and Engineering*, **33**, 427-437. https://doi.org/10.12989/gae.2023.33.5.427

[21] Garg, A. Shukla, N.K., Ramkumar Raja, M., Chalak, H.D., Belarbi, M.O., Tounsi, A, Li, L. and Zenkour, A.M. (2023) Finite Element Based Free Vibration Analysis of Sandwich FGM Plates under Hygro-Thermal Conditions Using Zigzag Theory. *Steel and Composite Structures*, **49**, 547-570. https://doi.org/10.12989/scs.2023.49.5.547

[22] Garg, A., Belarbi, M.O., Li, L., Chalak, H.D., Tounsi, A. and Zenkour, A.M. (2024) Comparative Study on the Buckling Analysis of Exponential, Power and Sigmoidal Sandwich FGM Plates under Hygro-Thermal Conditions. *Advances in Materials Research*, **13**, 431-462. https://doi.org/10.12989/amr.2024.13.6.431

[23] DiTaranto, R.A. (1965) Theory of Vibratory Bending for Elastic and Viscoelastic Layered Finite-Length Beams. *Journal of Applied Mechanics*, **32**, 881-886. https://doi.org/10.1115/1.3627330

[24] Mead, D.J. and Markus, S. (1969) The Forced Vibration of a Three-Layer, Damped Sandwich Beam with Arbitrary Boundary Conditions. *Journal of Sound and Vibration*, **10**, 163-175. https://doi.org/10.1016/0022-460x(69)90193-x

[25] Wilson, D.W. and Vinson, J.R. (1984) Viscoelastic Analysis of Laminated Plate Buckling. *AIAA Journal*, **22**, 982-988. https://doi.org/10.2514/3.8718

[26] Kim, C. and Hong, C. (1988) Viscoelastic Sandwich Plates with Crossply Faces. *Journal of Structural Engineering*, **114**, 150-164. https://doi.org/10.1061/(asce)0733-9445(1988)114:1(150)

[27] Huang, N.N. (1994) Viscoelastic Buckling and Postbuckling of Circular Cylindrical Laminated Shells in Hygrothermal Environment. *Journal of Marine Science and Technology*, **2**, Article 2. https://doi.org/10.51400/2709-6998.2483

[28] Pan, H. (1966) Vibrations of Viscoelastic Plates. *Journal de Mécanique*, **5**, 355-374.

[29] Librescu, L. and Chandiramani, N.K. (1989) Dynamic Stability of Transversely Isotropic Viscoelastic Plates. *Journal of Sound and Vibration*, **130**, 467-486. https://doi.org/10.1016/0022-460x(89)90070-9

[30] Zenkour, A.M. (2004) Buckling of Fiber-Reinforced Viscoelastic Composite Plates Using Various Plate Theories. *Journal of Engineering Mathematics*, **50**, 75-93. https://doi.org/10.1023/b:engi.0000042123.94111.35

[31] Zenkour, A.M. (2004) Thermal Effects on the Bending Response of Fiber-Reinforced Viscoelastic Composite Plates Using a Sinusoidal Shear Deformation Theory. *Acta Mechanica*, **171**, 171-187. https://doi.org/10.1007/s00707-004-0145-7

[32] Zenkour, A.M. and El-Shahrany, H.D. (2021) Hygrothermal Forced Vibration of a Viscoelastic Laminated Plate with Magnetostrictive Actuators Resting on Viscoelastic Foundations. *International Journal of Mechanics and Materials in Design*, **17**, 301-320. https://doi.org/10.1007/s10999-020-09526-6

[33] Zenkour, A.M. and El-Shahrany, H.D. (2021) Frequency Control of Cross-Ply Magnetostrictive Viscoelastic Plates Resting on Kerr-Type Elastic Medium. *The European Physical Journal Plus*, **136**, Article No. 634. https://doi.org/10.1140/epjp/s13360-021-01581-y

[34] Zenkour, A.M. (2022) Nonlocal Thermal Vibrations of Embedded Nanoplates in a Viscoelastic Medium. *Structural Engineering and Mechanics*, **82**, 701-711. https://doi.org/10.12989/sem.2022.82.6.701

[35] Sobhy, M., Zenkour, A.M. and Abazid, M.A. (2021) Hygrothermal Wave Dispersion Analysis of Metal Foam Microplates Strengthened by Graphene Embedded in a Viscoelastic Medium under 2D Magnetic Field Effect. *Mechanics of Advanced Materials*

and Structures, **29**, 7592-7604. https://doi.org/10.1080/15376494.2021.2003488

[36] Pham, Q., Ke Tran, V., Thanh Tran, T., Chinh Nguyen, V. and Zenkour, A.M. (2023) Nonlocal Higher-Order Finite Element Modeling for Vibration Analysis of Viscoelastic Orthotropic Nanoplates Resting on Variable Viscoelastic Foundation. *Composite Structures*, **318**, Article ID: 117067. https://doi.org/10.1016/j.compstruct.2023.117067

[37] Zenkour, A.M. and El-Mekawy, H.F. (2014) Bending of Inhomogeneous Sandwich Plates with Viscoelastic Cores. *Journal of Vibroengineering*, **16**, 3260-3272. https://www.extrica.com/article/15273

[38] Zenkour, A.M. and El-Mekawy, H.F. (2018) Stresses in Inhomogeneous Elastic-Viscoelastic-Elastic Sandwich Plates via Hyperbolic Shear Deformation Theory. *Journal of the Brazilian Society of Mechanical Sciences and Engineering*, **40**, Article No. 363. https://doi.org/10.1007/s40430-018-1284-4

[39] El-Mekawy, H.F., Hilal, M.O.S. and Zenkour, A.M. (2025) Bending Analysis of Different Types of Non-Homogenous Viscoelastic Sandwich Plates. *Journal of Applied Mathematics and Physics*, **13**, 797-820. https://doi.org/10.4236/jamp.2025.133041

[40] Illyushin, A. and Pobedria, B.E. (1970) Foundations of Mathematical Theory of Thermo-Viscoelasticity. Nauka. (In Russian)

[41] Pobedrya, B.E. (1977) Structural Anisotropy in Viscoelasticity. *Polymer Mechanics*, **12**, 557-561. https://doi.org/10.1007/bf00857005

[42] Allam, M.N.M., Zenkour, A.M. and El-Mekawy, H.F. (2009) Bending Response of Inhomogeneous Fiber-Reinforced Viscoelastic Sandwich Plates. *Acta Mechanica*, **209**, 231-248. https://doi.org/10.1007/s00707-009-0157-4

Appendix

The function $\pi(t)$ and $g_{\beta_m}(t),(m=1,2)$ can be determined by deducing the Laplace-Carson transform of these functions which are made with the known Laplace-Carson transform of the function $\omega(t)$, that can be written in the form:

$$\omega^*(s)=s\int_0^\infty \omega(t)\mathrm{e}^{-st}\mathrm{d}t \tag{A1}$$

Using Equation (28), one obtains

$$\omega^*(s)=s\int_0^\infty \left(c_1+c_2\mathrm{e}^{-\alpha t}\right)\mathrm{e}^{-st}\mathrm{d}t \tag{A2}$$

Then by integrating the above function, we get

$$\omega^*(s)=sc_1\left\{\left[\frac{-1}{s}e^{-st}\right]_0^\infty - c_2\left[\frac{1}{\alpha+s}\mathrm{e}^{-(\alpha+s)t}\right]_0^\infty\right\}=c_1+c_2s(\alpha+s)^{-1} \tag{A3}$$

But we have

$$\pi^*(s)=\frac{1}{\omega^*(s)}=\frac{1}{c_1+c_2s(\alpha+s)^{-1}} \tag{A4}$$

then

$$\pi^*(s)=\frac{\alpha+s}{c_1\alpha+s(c_1+c_2)}=\frac{1}{c_1}\left[\frac{c_1\alpha+c_1s+sc_2-sc_2}{c_1\alpha+s(c_1+c_2)}\right], \tag{A5}$$

or

$$\pi^*(s)=\frac{1}{c_1}\left[1-\frac{sc_2}{c_1\alpha+s(c_1+c_2)}\right]=\frac{1}{c_1}\left[1-\frac{1}{c_1+c_2}\left(\frac{sc_2}{\frac{c_1\alpha}{c_1+c_2}+s}\right)\right] \tag{A6}$$

Therefore, by using inverse Laplace Carson in the form, we find the function $\pi(t)$

$$\pi(t)=\frac{1}{c_1}\left[1-\frac{c_2}{c_1+c_2}\mathrm{e}^{\frac{c_1\tau}{c_1+c_2}}\right],\tau=\alpha t. \tag{A7}$$

Similarly,

$$g^*_{\beta_m}(s)=\frac{1}{1+\beta_m\omega^*(s)}=\frac{1}{1+\beta_m\left(c_1+sc_2(\alpha+s)^{-1}\right)},m=1,2 \tag{A8}$$

or

$$g^*_{\beta_m}(s)=\frac{1}{1+c_1\beta_m}\left[1-\frac{sc_2\beta_m}{\alpha(1+c_1\beta_m)+s\left(1+(c_1+c_2)\beta_m\right)}\right], \tag{A9}$$

and in the other form takes

$$g^*_{\beta_m}(s)=\frac{1}{1+c_1\beta_m}\left[1-\frac{c_2\beta_m}{1+(c_1+c_2)\beta_m}\left(\frac{s}{\alpha(1+c_1\beta_m)/\left(1+(c_1+c_2)\beta_m\right)+s}\right)\right] \tag{A10}$$

Then we can find the function $g_{\beta_m}(t)$ in the form

$$g_{\beta_m}\left(t\right)=\frac{1}{1+c_1\beta_m}\left[1-\frac{c_2\beta_m}{1+\left(c_1+c_2\right)\beta_m}\mathrm{e}^{\frac{-\left(1+c_1\beta_m\right)\tau}{1+\left(c_1+c_2\right)\beta_m}}\right], \tag{A11}$$

where $\beta_1=\dfrac{1}{2}$ and $\beta_2=2$.